Journal of Nuclear Materials 568 (2022) 153854

Contents lists available at ScienceDirect

Journal of Nuclear Materials

journal homepage: www.elsevier.com/locate/jnucmat

The TechnoFusion Consortium of Spanish institutions and facilities towards the development of fusion materials and related technologies in Europe

M. Gonzalez[a,*], R. Román[a], L. Bañares[b], M. Ferre[c], G. García[e], R. González-Arrabal[f], A. Ibarra[a], M.A. Monge[d], J. Olivares[g], J.M. Perlado[f], D. Rapisarda[a], F. Sánchez[a], J. Sanz[h], F. Seco[i], R. Vila[a]

[a] CIEMAT, Laboratorio Nacional de Fusión, 28040 Madrid, Spain
[b] UCM, Facultad de Química, 28040 Madrid, Spain
[c] Universidad Politécnica de Madrid, Centro de Automática y Robótica (CAR) UPM-CSIC, 28006, Madrid, España
[d] Universidad Carlos III de Madrid, Dpto. de Física, 28911 Leganés, Madrid, Spain
[e] Centro de Microanálisis de Materiales, Universidad Autónoma de Madrid, Campus de Cantoblanco, 28049 Madrid, Spain
[f] UPM, Instituto de Fusión Nuclear "Guillermo Velarde", 28006 Madrid, Spain
[g] CSIC, Instituto Óptica "Daza Valdés", 28006 Madrid, Spain
[h] UNED, ETS Ingenieros Industriales, 28040 Madrid, Spain
[i] UPM-CSIC, Centro de Automática y Robótica (CAR), 28500 Arganda del Rey, Madrid, Spain

A R T I C L E I N F O

Article history:
Received 4 January 2022
Revised 25 May 2022
Accepted 11 June 2022
Available online 13 June 2022

Edited by S Zinkle

A B S T R A C T

With the objective of contributing to the European development of materials, technologies and facilities for the demonstration of the thermonuclear fusion, the construction of the unique TechnoFusión facility was planned in 2009. The TechnoFusión consortium, formed by selected Spanish research groups and laboratories located in Madrid, has jointly advanced in the search for solutions to the remaining technological issues of nuclear fusion by magnetic and inertial confinement. In addition, the foundation of the TechnoFusión partnership has been essential to create a network of collaborations, and also to expand and specialize human resources, by training scientists and technical staff in the use of high-tech tools.

Supported by the TechnoFusión_Comunidad Madrid (III) regional programme, the consortium is focused on providing support for the construction of medium--sized, relevant facilities in Madrid (Spain). Regarding magnetic and inertial fusion issues, the programme is structured in several key experiments and infrastructures, which combine the development of materials, of cutting-edge technologies and the construction of associated facilities, with the progress in simulation and application of computational neutronics:

1. Introduction

The construction of a Spanish Scientific and Technological Singular Facility in the Community of Madrid, called ***TechnoFusion***, was proposed in 2009, where given aspects on the development of nuclear fusion-related technologies and facilities could be addressed. The facility will provide the Spanish Research Centers and Universities devoted to the development of Nuclear Fusion by magnetic and inertial confinement with a unique technological platform. Among them, the following areas were identified as needing long-term research and technological development: i) study of combined effect of neutronic radiation and intense magnetic fields in nuclear reactor materials, understanding the mechanisms of structural defect formation, the influence on materials properties of transmutation second products, and formulating more resistant alloys and functional materials; ii) interaction phenomena between nuclear plasma and the surrounding reactor devices by evaluating the synergies of high temperature, high flux and radiation combined actions; iii) liquid metals related studies, including the interaction with a free-surface liquid metal, as in DONES facility, and with fusion materials, and testing of extraction and purification systems; iv) robotic and remote handling experiments, to test and develop robotized systems for reactor repairing and maintenance tasks; and v) radiological risk evaluation, by developing the neutronic simulation tools to provide information about the activation of materials and reactor components and their decay times.

* Corresponding author.
E-mail address: maria.gonzalez@ciemat.es (M. Gonzalez).

https://doi.org/10.1016/j.jnucmat.2022.153854
0022-3115/

Since then, the TechnoFusión Consortium of Spanish Research Groups and Laboratories have jointly advanced, finding solutions for important infrastructures, training scientists and technicians in the use of high technology tools, and giving rise to a network of contacts and collaborations.

2. The TechnoFusion programme

The TechnoFusión programme is a Spanish research and development programme started on 2010. An initial group of researchers grouped together to provide support for the development of Fusion in Europe by launching the idea of a new singular scientific and technical facility. The consortium was then established as an association of researchers and engineers from the most important institutions, universities and laboratories located in Madrid, Spain, with an extensive background in the progress of fusion energy by magnetic and inertial confinement. The programme is based on the foundation of four consolidated fusion research and development groups, which carry out their activities at CIEMAT, UPM, UC3M and UNED, supported by the knowledge of groups at UCM and CSIC. The programme is specially supported by two laboratories of the REDLAB network of the Madrid Regional Government, which are decisive for the research in advanced materials operating under extreme conditions: the CMAM lab, a materials characterization facility using accelerated ion beams, and the LabMET, a scanning and transmission microscopy service. From the beginning, the programme and by extension the currently seventy-four participating people, is coordinated by the Fusion National Laboratory at CIEMAT while is economically supported without interruption by the Regional Government of Madrid, in Spain.

Organized around quite a number of scientific and technological objectives, the group of scientists and engineers of the TechnoFusión programme aimed to collaborate from a multidisciplinary approach towards the achievement of some of the issues currently raised in the field of fusion. More specifically, this third edition covering the period 2019-2022 is devoted to four main objectives: i) the design, production and improvement of advanced radiation-tolerant materials, complemented by the exhaustive material characterization, ii) the development of cutting-edge technologies, iii) the support on the construction of middle-size irradiation and testing facilities, and finally, iv) all accompanied with the advance of computational neutronic tools. The following sections will go briefly through selected tasks covered by the programme and their main experimental results.

3. The TechnoFusion scientific and technological structural objectives

3.1. Development of materials for ITER and DEMO

3.1.1. First wall materials

One of the development lines at the Universidad Carlos III, Madrid, Spain (UC3M, Dpto. Physics), deals with the production of first wall materials based on copper, copper-chromium-zirconium alloys (precipitation hardened material), and high entropy alloys, particularly towards the improvement of their thermomechanical behaviour as high heat flux components.

In order to investigate the powder metallurgical approach for the fabrication of new oxide dispersion strengthened Cu and CuCrZr materials, several alternatives have been investigated. It consists in the production of a fine dispersion of yttrium oxides in the CuCrZr matrix by milling yttrium (III) acetate tetrahydrate powders ($C_6H_9O_6Y{\cdot}4H_2O$ (Y3ATH)), thermochemically process the powders to decompose the Y3ATH, and finally sinter by hot isostatic pressing (HIP). The milling processing decompose the Y3ATH and the thermal treatment of the power under an Ar-10 vol% H_2 atmosphere eliminate the organic and volatile compounds and induce the formation of Y_2O_3 nanoparticles [1]. The ODS-Cu and ODS-CuCrZr produced following this powder metallurgy route have similar microstructures. After HIP, the microstructure of the materials is characterized by the presence of a dual microstructure of submicrometric and micrometric grains, having the submicrometric grains a higher density number of Y-O nanometric particles being identified as monoclinic Y_2O_3 by TEM analysis. The effect of different thermomechanical treatments, including hot rolling, in the microstructure and properties have been studied in the materials obtained under different variations of the production parameters [1–3]. This production route was firstly developed within Technofusion research programme to produce ODS-Cu reinforced by nanometric dispersion of Y_2O_3 [2,3]. Fig. 1 summarizes the mechanical and thermal behaviour (thermal conductivity, diffusivity and heat capacity) of Cu-ODS alloy at different temperatures.

The fabrication and characterization of an equivalent ODS-Cu alloy following a more direct powder metallurgy route has already been performed, starting from prealloyed powders CuCrZr with Y obtained from vacuum furnace induction melting followed by atomization in Ar [4]. The resulting materials exhibit good thermal conductivity.

The development of HEAs opens the possibility of achieving new materials with enhanced properties compared with those of the traditional alloys [5,6]. HEAs are composed of five or more elements in solid solution, which results in a high configurational entropy of the crystal lattice that may result in interesting properties such as "*self-healing*" after irradiation damage [7]. A new research line in the Technofusion programme is to produce and characterize reduced activation HEAs of interest for some of the fusion reactor components, such as the divertor, the plasma facing components and the structural components of the blanket [6,8], where enhanced materials are requested [9]. For example, the system CuCrFeVTi has been produced by arc melting, and the microstructure and mechanical properties have been characterized for $Cu_5Cr_{35}Fe_{35}V_{20}Ti_5$, $Cu_{10}Cr_{35}Fe_{35}V_{10}Ti_{10}$, $Cu_{15}Cr_{35}Fe_{35}V_5Ti_{10}$ and $Cu_{20}Cr_{30}Fe_{30}V_{10}Ti_{10}$ [10–12]. All the materials exhibit a dendritic microstructure and some degree of Cu and Ti segregation. The presence of a fine distribution of Cu nanometric particles, with a characteristic size of ~10 nm, was observed. This family of alloys are under research as a possible candidate for a compatible interlayer between the Cu-based cooling system components and the plasma facing materials. Other families of HEAs for structural applications, based in W, Ta, V, Ti, Fe and Cr have been produced and are currently under development in the UC3M research group [11,12].

3.1.2. Eurofer-based steels

Eurofer steel was a major breakthrough of the EUROfusion program and is the reference material for fusion structural applications. However, its use is limited to temperatures below 550°C for 20000 h. To improve not only the thermo-mechanical properties, but also the irradiation resistance, the UC3M group, is studying the material by optimizing its composition, production routes, and thermomechanical treatments. One of the results of this research line is the new oxide dispersion strengthened ODS-EUROFER obtained following a novel two-step powder-metallurgical route. Two batches of fine and coarse atomized EUROFER powders with addition of 0.4 wt.% of Ti and nanopowders of Y_2O_3 were processed separately. A final blend of the two batches was synthetized by HIP, obtaining a fully dense material [13]. The microstructure and mechanical properties in the temperature range RT-600°C were characterized. The steel exhibited a characteristic dual microstructure composed of zones with low and high density of carbides and nanometric Y_2O_3 oxides particles. The analysis of

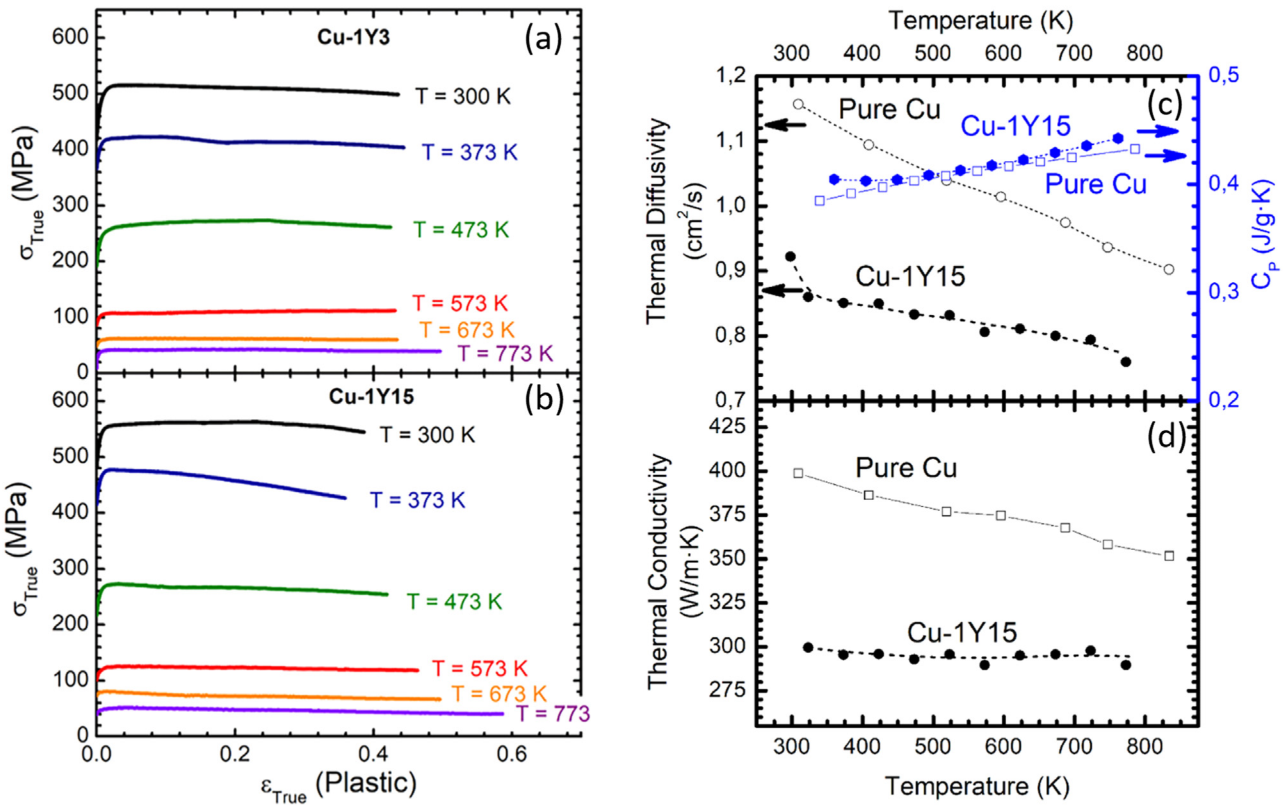

Fig. 1. True strain versus true plastic deformation of Cu- 1 wt% Y_2O_3 alloy: (a) Cu-1Y3 and (b) Cu-1Y15 obtained from compression tests at different temperatures. The difference between Cu-1Y3 and Cu-1Y15 is the time of the thermal treatment at 923 K under an Ar-10 vol% H2 atmosphere of the milled power before HIP sintering; 3 h for Cu-1Y3 and 15 h for Cu1Y15, respectively. (c) Thermal diffusivity and heat capacity, Cp of Cu-1Y15 compared with pure high thermal conductivity copper. The figures are from A. Muñoz et al. [2].

the EBSD measurements showed that the fraction of grains with a size smaller than 0.5 μm is ~23% (~19.2% ferrite and ~3.5% martensite) against ~17% (~15% ferrite and ~2.5% martensite) in the zones with lower density number of particles [13]. As Fig. 2 reveals, the novel ODS-EUROFER presents significantly improved tensile properties compared to commercial or new advanced steels developed for similar applications that have been submitted to specific thermo-mechanical treatments to optimize their properties. The deformation mechanism responsible of the enhanced mechanical properties of the steel was explained through EBSD experiments. Preliminary results depicted in Fig. 2(c) demonstrate that this new ODS EUROFER might further improve its mechanical properties after adequate thermomechanical treatments, such as hot forging or rolling.

Other ODS-reduced activation ferritic steels (RAF) have been developed within the Technofusion programme by the UC3M group [14]. The development of thermomechanical treatments to improve the mechanical properties and irradiation resistance of the produced steels is also addressed. As an example, the results reported by Oñoro *et al.* [14] showed that the Fe–14Cr–2W–0.4Ti-0.3Y_2O_3 (wt. %) increases the ductility and the yield strength after hot cross rolling (HCR) followed by an annealing treatment at 1273 K. The microstructure is characterized by submicron sized elongated grains with a high density of Y-Ti-O nanoparticles, Cr-W-rich precipitates and Ti-rich oxides (see Fig. 3). The resistance to thermal fatigue and aging were also studied by submitting a batch of samples to thermal cycling between 773 K and 1073 K and another batch to aging for 2000 h at 873 K. Both treatments resulted in an increase in hardness without a substantial effect on the tensile or yield strength [14].

To simulate the effect of a fusion environment at different doses and temperatures, the resistance to the irradiation damage of different ODS RAF steels produced by the group of UC3M has been analyzed by ion implantation of He^+ and Fe^+ at the Centre for Micro Analysis of Materials (CMAM) in collaboration with CIEMAT. Single and sequential implantations of He^+ and Fe^+ ions in Fe-14Cr-2W-0.3-Ti-0.3Y_2O_3 (wt%) subjected to different production routes and thermomechanical treatments (HCR or hot forging) were investigate. The results were compared with those obtained for a model Fe14Cr alloy ion implanted under similar conditions (see references [15] and [16] for more details on implantation energies, temperatures and doses). The vacancy-type defects and bubbles produced by the irradiations have been characterized by slow Positron Annihilation Spectroscopy (PAS) and Transmission Electron Microscopy (TEM). The analysis of TEM results have shown that under the studied irradiation conditions there are no significant changes in the mean size, qualitative chemical composition and density of the reinforcing nanoparticles, merely a slight coarsening of the smaller nanoparticles. The formation of very small bubbles with sizes below ~2 nm was observed in all the steels after He^+ irradiation mainly in the ferritic matrix, regardless of the irradiation temperature from RT to 450°C. A lower bubble density is formed in the ODS steels compared to the model alloy, where bubbles with an average size ~30 % larger were observed [15,17]. This result points out the higher radiation resistance of the ODS steels compared to not reinforced steels. PAS experiments reveal that He^+ irradiations introduce changes in the chemical environment of open-volume positron traps, possibly due to the creation of He-vacancy complexes [15,16].

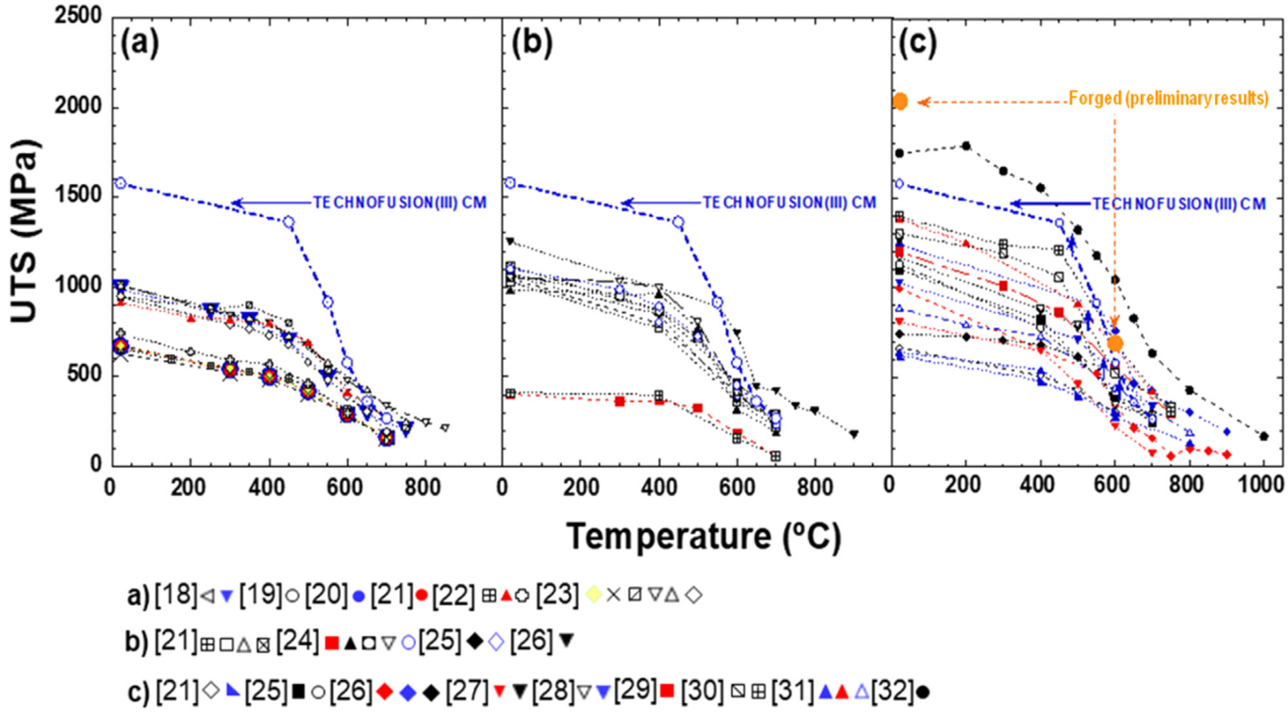

Fig. 2. UTS as a function of temperature for the new ODS-Eurofer in the as HIP state compared with various steels for similar applications. (a) Eurofer and ODS Eurofer steels, (b) high Cr ODS steels and (c) high Cr ODS steels with subsequent thermomechanical treatments (modified figure from [10]). See reference [10] for the cross references included in this figure.

3.1.3. Corrosion protection and antipermeation coatings

The development of appropriate BBs requires, among other R&D activities, the fabrication of multifunctional coatings which act as: (i) barriers for tritium permeation (ii) anticorrosion agents against the action of Li, (iii) walls that prevent the diffusion of the Li contained in the breeder towards the steel, and (iv) in the case of the magnetic fusion, as insulators to avoid magneto hydrodynamic (MHD) effects in the self-cooled liquid metal approach.

In the Technofusion frame, the corrosion behavior of bare Eurofer steel and of several coatings (nanostructured W, SiC and Al_2O_3) sputtered on Eurofer substrates [18] has been studied under similar conditions to those that would take place in the helium cooled pebble bed (HCPB) breeder concept. Corrosion tests were carried out by exposing the samples to the presence of ceramic pebbles, whose composition was a mixture of lithium silicate/titanate prepared by Karlsruhe Institute of Technology (KIT), for 240 h at a temperature of 550 ºC under a He/H_2O purge gas mixture [19]. SEM and EDX data for the tested bare Eurofer evidence the presence of a surface layer with a thickness of ~2 μm, a double corrosion layer formed by a Fe-rich sublayer located close to the sample surface, and a Cr-rich sublayer is found underneath. This corrosion layer can modify the bare Eurofer behavior and be strongly relevant under irradiation.

3D topography images for a nanostructured W (nW) coating show its partial lost during the corrosion test. XRD data evidence that the remaining nW layer has oxidized, forming WO_3 and $FeWO_4$ phases. Because of oxidation and its derived problems, the use of nW as corrosion barrier in the HCPB concept is excluded. 3D topography and SEM images for the tested Al_2O_3 coating indicate that the corrosion test has increased the surface roughness without notably modifying the coating morphology along its thickness. XRD patterns for this sample illustrate the formation of a $LiAlO_2$ phase during the test meaning that Al_2O_3 has reacted with lithium contained in the pebbles (Fig. 4). Indeed, SIMS data show that lithium homogeneously distributes along the whole thickness of the tested coating up to first layers of the Eurofer substrate underneath. SiC coatings have been demonstrated to be very stable with exceptionally low chemical reactivity with lithium. They have satisfactorily withstood the corrosion test, acting as a real barrier to lithium and protecting the Eurofer against corrosion.

Therefore, the performance as deuterium permeation barriers of these SiC coatings was studied in terms of the influence on permeation values of the: (i) thermal cycling at 450°C, (ii) combined thermal cycling and electron irradiation (1.8 MeV up to a total dose of 1 MGy), as well as (iii) oxygen exposure at a temperature of 450°C during electron irradiation. Data show that the permeation reduction factor (PRF) for the as-deposited SiC coated is $\sim 10^4$, even at breeder operational temperatures. Thermal cycling leads to a rearrangement of the amorphous structure and slightly reduces the PRF value (less than one order of magnitude). The effect of electron irradiation in the PRF is very small at the selected conditions during thermal cycling. However, the exposure to oxygen at 450°C during electron irradiation leads to the oxidation of the coating surface and reduced the PRF by about three orders of magnitude [20].

D retention and desorption in SiC coatings were also tested. Coated samples were implanted with 7.5 keV D prior to or after being submitted to the treatments previously described. SIMS data show that in all implanted coatings D is retained in the implantation region and is mainly desorbed at temperatures larger than ~ 800°C. Prior to implantation, thermal cycling increases the density of dangling bonds, enhancing D retention in the coatings and leading to the appearance of a second D_2 desorption peak at lower temperatures (~400-750°C). Electron irradiation during thermal cycling does not considerably change the D retention but the low temperature D_2 desorption peak is shifted to higher temperatures (~500-750°C) because of the ionizing effects [20].

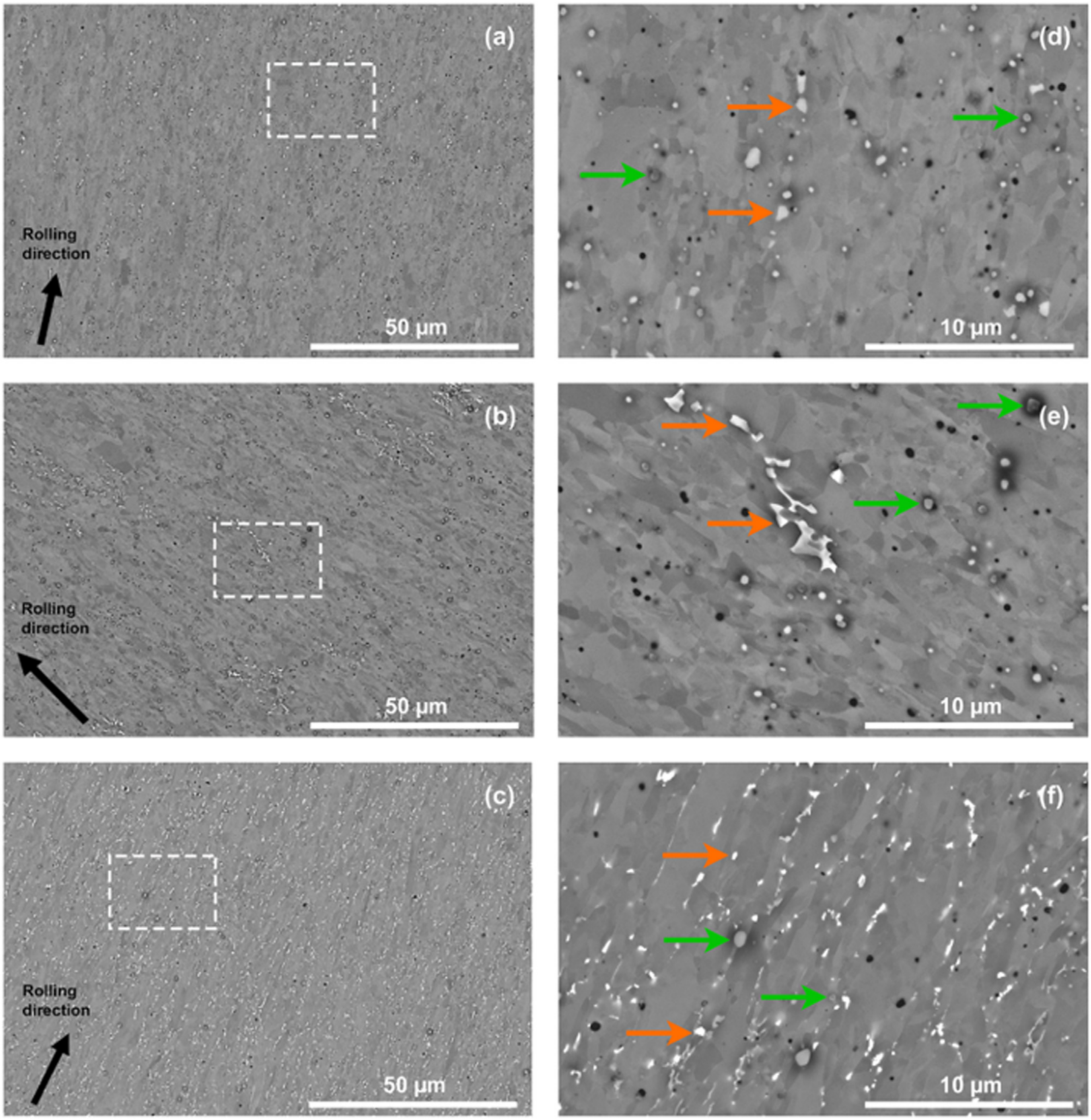

Fig. 3. BSE SEM images of Fe14Cr2W0.4Ti-0.3Y_2O_3 (wt. %) after (a) hot rolling and thermal annealing at 1273 K, (b) thermal cycling test (100 cycles between ~673 and 1073 K) and (c) thermally aged at 873 K for 2000 h in Ar protective atmosphere. (d), (e) and (f) show zoom-in images from white squared areas in (a), (b) and (c), respectively. Cr-W-rich precipitates (orange arrows) and Ti-rich precipitates (green arrows) are highlighted (figure from reference [11]).

3.1.4. Materials for optical applications

Finding materials with high transmittance and radiation tolerance is of vital importance for fusion applications. So far, the considered options show a strong decrease in optical properties after neutron irradiation. Within TechnoFusion and EUROfusion programs, sapphire, spinel ($MgAl_2O_4$, both single and poly-crystals), amorphous silica, calcium and barium fluorides (for IR applications) and yttrium aluminum garnet (YAG) have been the materials chosen at CIEMAT for optical components with applications as windows, LEDs or optical fibers. Samples from different manufacturers have been compared. Experimental measurements include optical absorption on samples irradiated with neutrons at doses from 0.1 to 1 dpa (10^{21} n/cm^2), together with the unusual method of measuring samples also under gamma radiation, to quantify the expected effect in more real fusion operating conditions (neutrons + gamma damage).

One of the first results that should be particularly highlighted is to have verified that for all materials the optical absorption is clearly underestimated when measuring only neutron post-irradiated samples, because ionizing radiation increases the absorption. This gamma effect disappears at room temperature after some recovery time, being the reason why the time elapsed between removal from the fission reactor and the optical measurement (usually quite long) reduces the absorption. Furthermore, the optical damage is not linear with neutron dose, but saturation is already observed at 0.4 dpa, especially for the transparency loss of

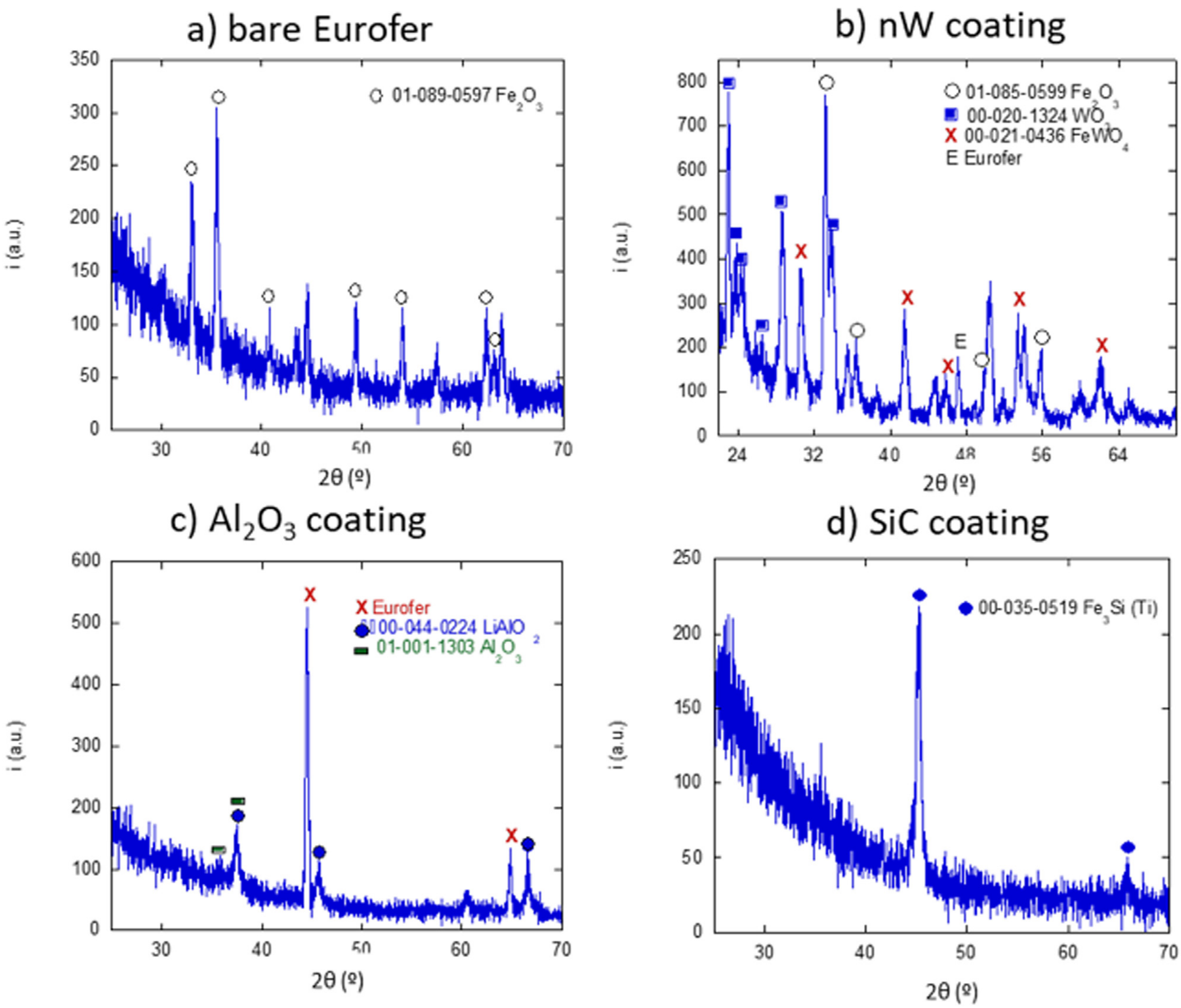

Fig. 4. XRD spectra for the bare Eurofer (a) and for the diverse coating sputtered on Eurofer after the corrosion test: nanostructured W (nW) (b), Al2O3 (c) and, SiC (d).

silica and is also retained at 1 dpa. Finally, silica seems to be the ideal material for optical properties in fusion environments, being the most radiation resistant material of those tested so far, showing an unusual resistance behaviour.

3.2. Cutting-edge technologies

3.2.1. Ion-irradiation related technologies

There are currently no facilities where materials can be tested under fusion reactor conditions and neutron radiation must therefore be simulated using other methodologies. One experimental way of approaching the study of the effects of neutron radiation on materials is by means of ion beam irradiations. This methodology has advantages and disadvantages, but its application in the framework of EUROfusion in structural and even functional materials is accepted and recommended. TechnoFusión Programme counts with a powerful partner: the Centre for Micro Analysis of Materials (CMAM) a research center at the Universidad Autónoma de Madrid devoted to the analysis and modification of materials by means of a 5 MV electrostatic ion accelerator [21]. In particular, an experimental chamber for the irradiation and implantation of materials is available for materials for fusion testing in the accelerator facility. The chamber includes a beam degrader to simulate a more homogeneous implantation profile and therefore the volume of structural damage. Among the studies carried out so far, the irradiation of ceramics for breeder blanket applications is here selected to illustrate the practice with accelerated beams using such energy modifying device [22,23]. The beam degrader was used to homogeneously implant light ions in breeding blanket ceramics, simulating the generation of T and He as a result of neutron-induced lithium transmutation. As an example, Fig. 5 depicts the SRIM simulation of proton induced-damage (in dpa) and concentration (in appm) maxima along the irradiated thickness of a 4.5 MeV H^+ irradiated alumina sample. The irradiated probe was afterwards tested, and comparatively studied with probes in the as-received condition, obtaining encouraging results about the material radiation and mechanical resistance. At least up to a total fluence of 1.0×10^{16} ions/cm^2, SEM observations [22] and cross-sectional indentation results (Fig. 5) indicate that these 99.7% pure commercial alumina is not affected by proton implantation, while the four-point bend tests conclude a decrease in the compression strength after irradiation [22]. Due to the larger area in comparison with the bulk of the thin sample, the noticeable roughening induced in the two surfaces of beam incidence likely affects reducing the resistance to bending.

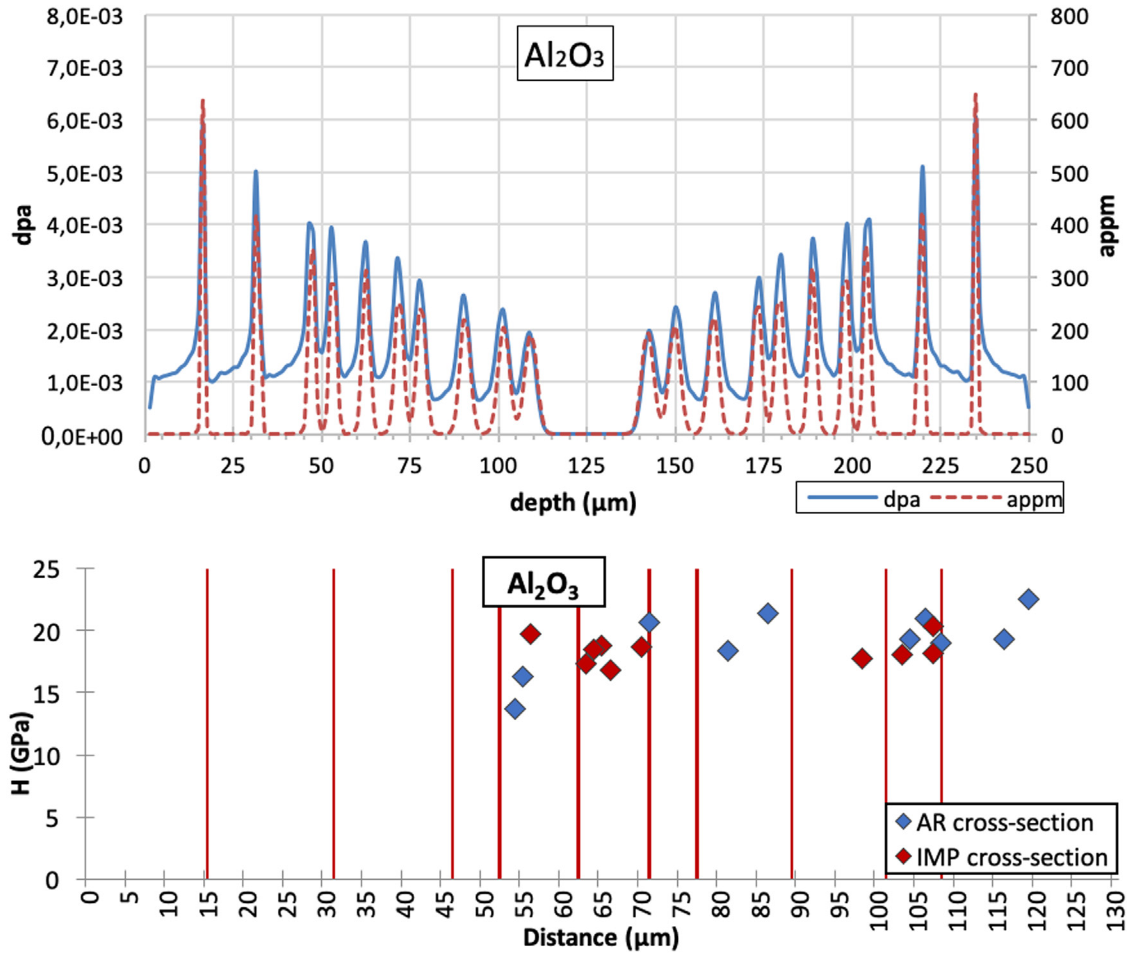

Fig. 5. High energy proton irradiation on an alumina thin probe. A beam degrader and the ion impinging from both probe surfaces was used to achieve a bulk homogeneous implantation. Top plot, the SRIM simulation of radiation damage (in dpa; solid blue line) and hydrogen-implanted concentration (in appm; dashed red line) as a function of specimen thickness. Bottom plot, hardness values calculated at different depths in alumina from cross-sectional, Vickers-type indentation tests. Red vertical lines represent the ionic stopping range when using the beam degrader. Blue and red diamonds correspond to as-received and ion-implanted samples, respectively.

3.2.2. Remote handling

Within the TechnoFusión Programme, important support is being given to the development of remote handling technologies, as one of the main pillars of activities in radiation facilities. The remote handling (RH) with the aid of a robot (*the slave*), controlled by a human-through-control device (*the master*), presents advantages in situations of dangerous environments or places with difficult access of non-repetitive tasks, examples of conditions perfectly achieved in IFMIF-DONES facility [24]. The process of implementing a RH system can be structured in several steps: i) the development phase, starts when a new requirement is determined, ii) the design of the software and hardware procedures, iii) the building and codification of the system, and finally iv) the testing, which, depending on the success, determines if the system can be deployed in the operational phase. In IFMIF-DONES, two good examples of situations where RH is of paramount importance are the repair and replacement of components in the Test Cell and the Beam Transport Room, because of the high radiation doses and the difficult access [25]. Special cranes are under development to be adapted to the facility components geometry. Thanks to adaptors and effectors, the Heavy Rope Overhead Crane (HROC) and the Access Cell Mast Crane (ACMC), as an example, are able to perform the lifting, positioning and guiding of the Target Assembly components out of the Test Cell or place them back inside. One of the main challenges to face is the radiation resistance of RH components. To anticipate the radiation tolerance of a three degree-of-freedom robotic arm, the response of the included microcontroller and micro servo-motors moving the three rotational joints has been monitored by the RH group at the Universidad Politecnica of Madrid during ionizing radiation testing at CIEMAT. The required radiation conditions were achieved by means of the Bremsstrahlung radiation caused by a high current, 2 MeV electron beam striking an aluminum sheet. The plots on Fig. 6 show the motors trajectory while receiving a radiation dose up to 0.18 Gy/s. Clearly, the robot loses precision over time. The positioning error becomes more noticeable from minute 35, and the robotic trajectory starts to be different after 40 minutes of irradiation. The analysis indicates a possible internal leakage current due to the increase of temperature and current, and therefore shielding the electronic components to increase the IC radiation protection will be needed.

3.2.3. Safety of radiation facilities

The Indoor Positioning System (IPS) is here chosen as another example of the engineering developments addressed in the framework of TechnoFusión Programme due to requirements of high-level radiation facilities. In IFMIF-DONES, the aim is to determine the location of the facility staff at all times, to ensure that workers have left the restricted areas before the start of the operation, and to better estimate the total radiation dose annually received by workers, without providing information for surveillance purposes (visual or otherwise) about the activities carried out by workers.

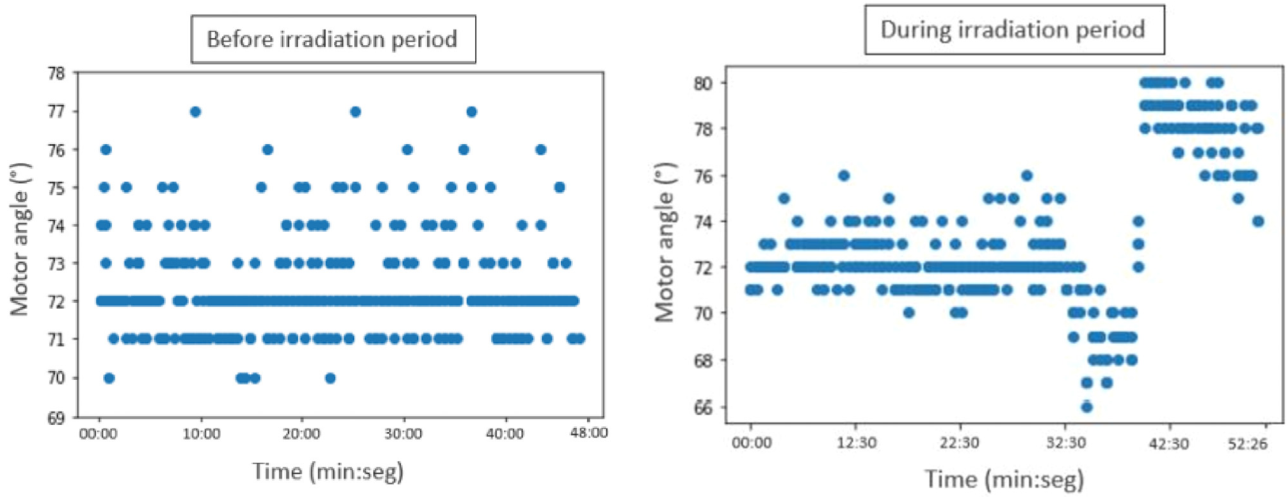

Fig. 6. Behaviour and response of a three-degree-of-freedom robotic arm under an ionizing radiation field. Plots of trajectory evolution of a rotational servo motor, where a positioning error is noticeable from minute 30, the robotic trajectory becoming odd after 40 minutes of irradiation.

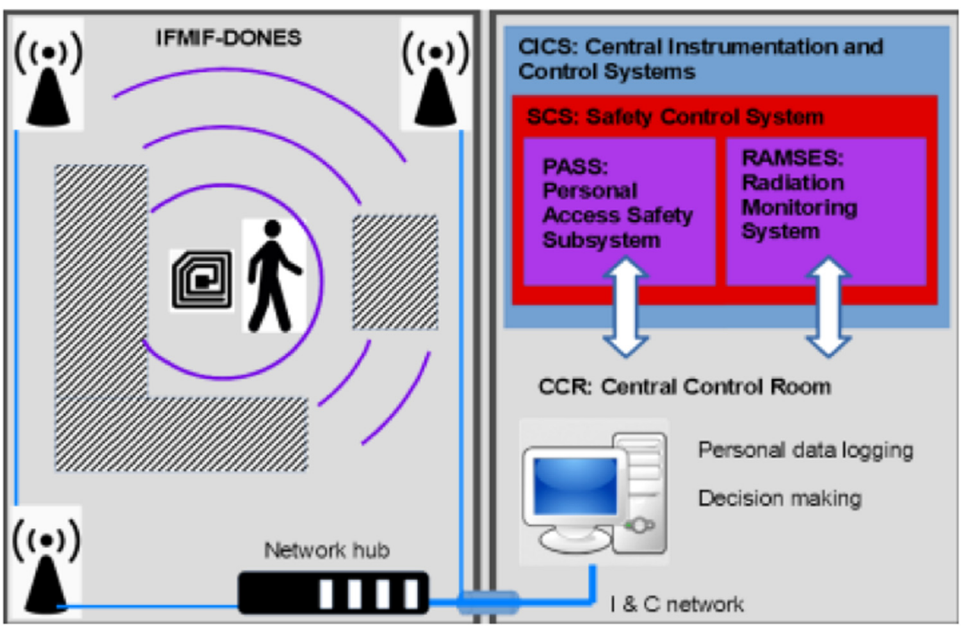

Fig. 7. Configuration scheme of an indoor position system for human safety evaluation within a radiation facility such as IFMIF-DONES.

The IPS consists of a number of active radiofrequency tags worn on workers' clothing, periodically emitting identification codes. A network of radiofrequency (RF) readers located in the monitored areas will detect the presence of the RF tags and therefore will estimate the location of the radiation exposed people (Fig. 7). The measurements will be transmitted via a local communications network to a central point where all the information is collected and displayed [26]. Simulation tools are needed to determine the coverage and the reliability of the tracking system. The thick shielding concrete calculated for the facility is considered one of the great challenges of the location system in IFMIF-DONES, as it implies a great attenuation of the RF signals. In consequence, a simple IPS system with a proximity location system is envisaged, in which the location of the users is estimated with room-level accuracy. Given previous uses in another nuclear facility, the radiofrequency identification (RFID) technology is considered a good choice to support the IPS. A second challenge is the background radiation existing in frequently accessed and restricted access areas; in these areas, the resistance of the electronic positioning systems to the radiation generated must be studied, and protective shielding must be designed to prolong their useful life. Considering expected radiation levels of approximately 10 mGy/h, preliminary studies show that the (unprotected) RF readers or tags could have an expected lifetime of several months.

3.3. Support to construction of medium size experimental infrastructures

3.3.1. The liquid metal laboratory

There are several facilities under design or construction in which the TechnoFusión programme is contributing. In the Liquid Metal Laboratory at CIEMAT, two experimental PbLi loops so far commissioned are under further development for testing fusion-related technologies.

CiCLo, the first corrosion experiment for structural and functional material testing under dynamic conditions [27] was de-

Fig. 8. On the left, a picture taken of CiCLo, the CIEMAT PbLi corrosion loop for testing of materials and corrosion protecting coatings. Also located at CIEMAT, the image on the right depicts CLIPPER, the PbLi loop designed for validation of permeation technologies.

signed aiming to test structural but also functional materials and coatings (Fig. 8). Besides, the loop will allow the understanding of relevant parameters related with chemical compatibility of materials and liquid PbLi, e.g. the influence of impurities and corrosion residues and their concentration. With a capacity of approximately 7 liters, the isothermal, electromagnetic pumped, PbLi loop operates at fusion relevant temperatures and liquid metal velocity (1 m/s). In CiCLo, the alloy is melted in a separate tank inside a glove box under controlled atmosphere, from which the liquid metal is transferred to the storage tank. A permanent magnet electromagnetic pump (PMEP), working up to 600 ºC and supplying different flow rates, forces the liquid metal motion through the test section. An electromagnetic flowmeter is set to record and monitor the flow rate. The loop has an expansion tank to support liquid volumetric variations and outgassing. The entire loop is connected to a parallel argon circuit to ensure emptying and filling operations. The experimental section has been designed for the samples to be easily removed.

CLIPPER, another isothermal forced circulation PbLi loop (Fig. 8), was built to fully characterize representative technologies for the liquid blanket concepts [28]. The loop is described by a variable mass flow rate (2-39 kg/s), velocities up to 1 m/s and temperatures between 300 and 500ºC. The metal is heated, melted and cleaned in a tank located outside the loop and integrated in a dedicated glove box under argon atmosphere. The melted PbLi is then sent to the storage/filling tank before entering the loop. After the PMEP, the upper part of the loop allocates the flowmeter followed by the expansion tank and the gas injection system. Then the PbLi circulates through the gas extraction system prototype to finally reach the PMEP. So far, different prototypes of T extraction by the permeation against vacuum (PAV) technology are being fabricated at CIEMAT to be coupled to the experimental loop [29]. The PAV technology is based on the diffusion of hydrogen isotopes through vanadium permeable membranes supported on a steel structure and affected by a pressure gradient. A complete characterization of the membrane has been performed in terms of permeability [30], mechanical properties and welding procedures. Due to leaks found in the first prototype, two new manufacturing approaches are being considered: i) the use of electron beam welding or ii) the avoidance of welding using specific gaskets. For permeation tests, H or D needs to be solubilized in the liquid PbLi to simulate the neutron production of tritium in the breeding blanket. A gas injection system based on forced permeation was proposed to be installed in the loop. The first prototype is actually under fabrication using permeable niobium membranes in a tube-in-tube steel component [31].

3.3.2. The CIEMAT's triple ion facility

To advance in the knowledge of the irradiation effects while fusion-neutrons facilities like IFMIF-DONES are under design or construction, high-energy ions are a reasonable approximation to study the damage rate and the generation of the transmutation products in structural and functional materials. Simulating the effects of neutron irradiation by means of in-confluence multiple ion beams presents some important advantages compared to neutron irradiation. Among them, i) high damage rates and implantation doses are achieved in short periods of time, and ii) ion irradiation allows the safe handling of reduced activated samples for their direct characterization. Nevertheless, ion beams are severely limited in the acceleration energy and therefore in their penetration depth into the target material.

To cover the deficiencies of the actual triple ion beam facilities, CIEMAT has launched a project to construct an irradiation facility of two Tandem linear accelerators and a high energy cyclotron, for the implantation of light ions and the acceleration of heavy ions towards the same target simultaneously. The CIEMAT's Ion Device (CID) facility has been designed to produce neutron comparable effects, its most relevant feature being the possibility of modifying the induced damage rate and the total dose of light ion implantation by several orders of magnitude, having full control on current and dose during irradiation. The use of beam energy degraders will allow the homogeneous irradiation of volumes (20-30 microns in depth) on temperature controlled targets. Besides, several solutions are being considered to mitigate the impurification of samples during ion irradiation, specially with carbon: i) the clever use of magnets to produce the cleanest beam, ii) the installation of cold traps near the sample, iii) the deposition of thin film (when possible) on sample surface, or iv) the use of plasma cleaners, some of which have been already suggested by G. Was [32].

Fig. 9 shows the 2D distribution of accelerators, ion transmission lines and experimental chambers of the triple beam facility housed inside an emblematic CIEMAT building and distributed over four floors. The second floor will store the ion sources for the tandem accelerators, which will be placed in vertical position in the first floor. The experimental room for horizontal irradiation with double or triple beams will be located on the ground floor, leaving the basement floor to carry out vertical triple beam irradiations, for example microstructural observation in real time by installing a TEM.

The facility will be developed in two phases. The first one will involve the location of two tandem accelerators with the capacity to accelerate light ions (H, D or He) up to 18 MeV and 40μA, and iron and heavy ions up to 50 MeV and 3 μA. In this situation, the

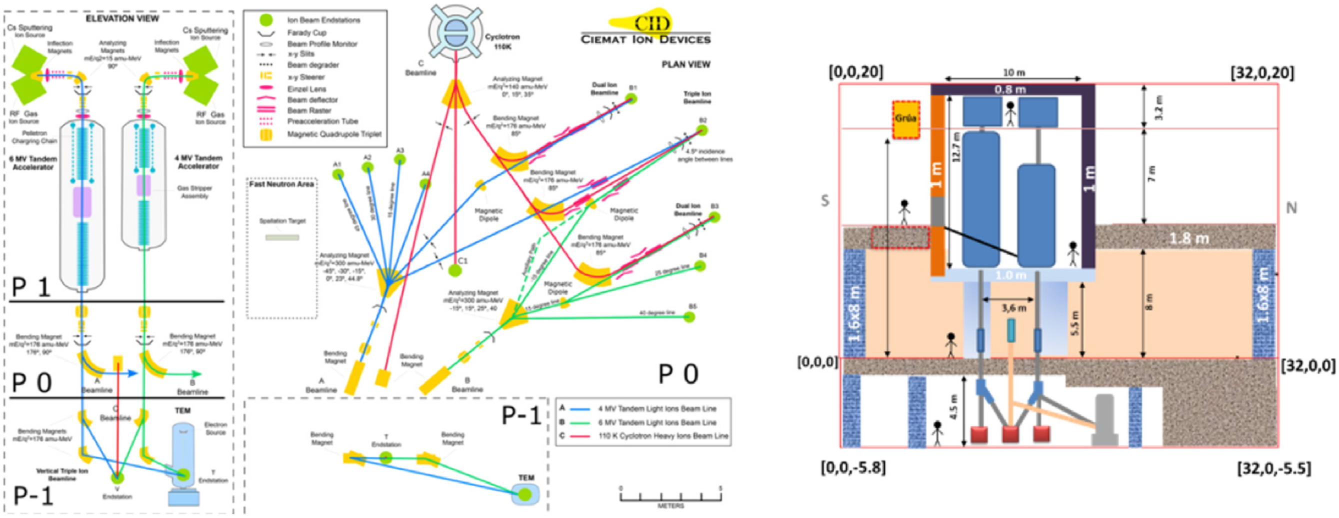

Fig. 9. The four-story distribution of ion accelerators and experimental chambers at the CID in-confluence triple ion beam facility.

facility will be operational for simultaneous irradiation with two beams. In a second phase, the facility will be completed with a high energy cyclotron with currents up to 10 µA (Fe+4) to achieve the in-confluent triple ion beam irradiation of Fe, He and H ions on a steel target. The maximum penetration range in iron is calculated to be 25 µm.

3.4. Computational neutronics and simulation

The TechnoFusion Programme is accompanying the development of computational neutronics, which is essential for the optimum design of all-sized facilities and components. Computational neutronics enables to perform nuclear analyses in support of the design, commissioning, and operation of nuclear facilities. Facilities which are or will be complex, have a high degree of material heterogeneity and a very large number of radiation streaming paths, with radiation sources that are complicated to simulate. The need for high-fidelity and high-resolution results has driven impressive advances in computational radiation transport and activation. Efforts are being conducted worldwide to improve and evaluate computational models and data so that reliable nuclear design and performance analyses can be done for future fusion devices.

The main objective of this section is to present the progress achieved within the group of engineers and physicists from UNED and CIEMAT in the development of the computational tools to address the two main subjects of fusion neutronics:

- Radiation transport, to characterize and analyze the radiation fields of possible radiation sources (e.g. neutrons, protons, deuterons) and the related nuclear responses.
- Coupled transport-activation calculations, to determine the isotopic inventory and activation of real components in current scenarios, compute the generated decay-radiation and perform radiation transport and decay nuclear response calculations.

Besides, some comments will be made to illustrate their suitability for fusion neutronics calculations when applying to nuclear analysis and design of ITER and DONES, as well as DEMO or future power plants.

3.4.1. Advanced computational methods and tools for neutronic analysis of fusion technology systems

The calculation workflow for advanced CAD-based Monte Carlo (MC) transport and activation simulations as used at UNED is schematized in Fig. 10, where the computational tools and the developed code systems are represented. For geometry modelling, the Constructive Solid Geometry (CSG) approach is followed. GEOmetry-UNED (GEOUNED) is a tool recently developed at UNED to automatize the translation process of a CAD engineering model into the CSG representation, as routinely used in Monte Carlo transport codes, such as Monte Carlo N-Particle (MCNP). In all these tools, the automatic void generation represents a critical feature in the geometry conversion of highly complex models, as is the case of ITER. GEOUNED has made a difference in this issue, introducing the capability to use complex nested enclosures, which generates structured hierarchical voids producing cleaner and human-readable inputs [33]. It is worth noting that the generation of a similar void structure with other conversion software tools requires a tedious process that implies several runs and user intervention, while GEOUNED makes it automatically in a single run.

For particle (neutron, light ions) and photon transport simulations, the MCNP 6.2 code is UNED's basic computational tool. However, relevant extensions of the native code have been developed to satisfy ITER and in general fusion neutronics needs. This enhanced version, called MCUNED-Plus, is designed to address transport and coupled transport-activation calculations by assembling and extending capabilities of the previous Monte Carlo-UNED (MCUNED) [34] code and the transport codes of Rigorous Two-Step-UNED (R2SUNED) [35] and Direct One-Step-UNED (D1SUNED) [36] systems as follows:

1.- Optimization algorithms, by modifying the loading, storing, and plotting native MCNP routines, have been developed to manage the increasingly complex geometry models [37]. Great improvements have been achieved in RAM memory saving (80%) and reduction of loading time (98%) for model initialization. Furthermore, the new algorithms enable a more efficient ray-firing process of determining the next geometrical cell boundary (20% simulation speed up, ITER C-lite model) and a faster visualization (easy geometry checking for lost particles) [36,37].

2.- New tally capability, called Cell-under-Voxel (CuV), enables differentiation of materials and fluxes within the voxels of a structured mesh. For voxels containing different materials, CuV generates a different tally for each material corresponding to the real flux, not to a voxel-averaged flux. Originally developed for capturing gradients in the neutron flux [35],

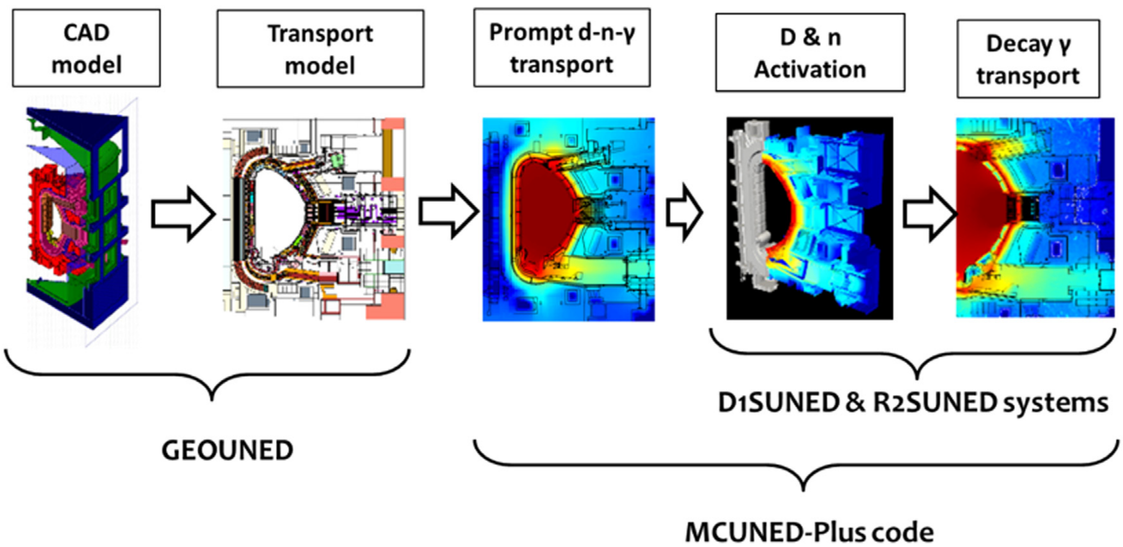

Fig. 10. The workflow and simulation tools followed by the neutronics group at the UNED, Madrid, Spain.

this technique can be routinely used when a high-resolution and accurate representation of a nuclear response throughout a heterogeneous geometry is demanded, such as nuclear heating as source term in thermal analysis.

3.- Ability to provide time-integrated radiation fields and dose mapping from moving radiation sources.
4.- A variance reduction process has been implemented to bias the nuclear interaction of charged particles during the transport, increasing significantly the number of secondary particle tracks produced during the simulation while allowing a good simulation statistics where the transport of secondary particles (neutrons and photons induced by charged particle reactions) is of interest.
5.- The implementation of a new kinematics for the angular distribution of neutrons produced by a deuteron breakup reaction. The current formulation implemented in MCNP is not able to reproduce the experimental angular distribution peaked forward to the direction of the incident deuteron.
6.- Specific developments for source modelling (volumetric and surface sources). Two illustrative examples are the one to provide maps of source importance to specific target tallies, and other to filter (tally/meshtally) by source components.
7.- Extensions to implement the Rigorous Two-Step (R2S) and the Direct One-Step (D1S) methodologies for residual fields calculations of decay photons, neutrons, and photoneutrons from neutron and proton/deuteron-induced activation.

One of the most complex problems in fusion neutronics is the determination of the radiation fields after shutdown, mainly due to the decay photons emitted by radioactive nuclides produced by the activation of materials during facility operation. Activation, decay heat and shut-down dose rate (SDDR) analyses are an important input in the nuclear design on any fusion device. Two approaches have been proposed to address the problem.

The R2S methodology, implemented at UNED into the R2SUNED code, involves neutron and decay photon transportations, performed with MCUNED-Plus transport code and ACtivation ABacus Code (ACAB) for activation calculations [38]. Simulations are done separately, coupled by a nuclear inventory analysis code, using suitable interface scripts of general application, although having some accuracy limitations. Transport by MC enables the geometry to be represented continuously, but a discrete characterization (mesh-based description of materials) is required, which set limits to the accuracy. The limitations due to the spatial gradients of the neutron flux and the decay gamma source can be overcome with the CuV technique, which does not require to use a conformal mesh. Furthermore, a dedicated methodology was implemented into the R2SUNED code to enable the propagation of errors over the whole calculation sequence, from neutron transport over the activation calculations to the decay photon transport [39]. Maps of decay gamma source importance to specific target tallies, estimation of the radionuclide's contribution to residual dose, and estimation of the production pathways contribution for the most relevant radionuclides are some of the analysis capabilities provided by R2SUNED.

The other approach, the so-called D1S, performs both the neutron and decay-photon transport simultaneously in the same MC simulation. Where a linear dependence between the activity of all the radioisotopes of interest and its production rate is valid, D1S is the most accurate approach since no discretization is needed for any variable. This approach is implemented at UNED into the D1SUNED code system, being MCUNED-Plus code its main software element. It includes pioneering capabilities to address the large variety of SDR problems of fusion facilities by efficient calculation and suitable analysis of the results. D1SUNED also includes a software of reference that enable production of the D1S dedicated activation/transport libraries needed to run transport calculations [36,40]. Activation pre-analysis to know the most important radionuclides and activation cross sections are performed with the ACAB code.

The updated R2SUNED and D1SUNED code systems enable the calculation of decay gamma fields produced by both charged particles [41] and secondary neutron activation. As for D1SUNED, this calculation can be carried out in a single coupled charged particle-neutron-decay gammas simulation. The suitability of R2SUNED and D1SUNED is widely demonstrated in applications to ITER, DEMO, IFMIF-EVEDA and DONES. Furthermore, the codes were benchmarked through an ITER-oriented exercise and validated for an ENEA Frascati Neutron Generator 14 MeV neutron irradiation experiment and JET dose rate measurements (D-D, D-T), demonstrating a comparable behavior to similar European tools. D1SUNED is the reference code system in ITER and the CuV R2SUNED approach is fully compatible with the unified European R2S code system, called cR2S (common R2S), under development by CCFE, KIT and UNED within EUROfusion.

3.4.2. Applications to nuclear design and performance analyses

An illustrative example of the suitability of these neutronics developments to ITER analyses is that UNED has produced the official radiation atlas in 2016 and 2020 to demonstrate compliance with regulatory limits [42,43]. Some of the most complex and sophisticated MCNP models ever built were created in the framework of ITER and have been efficiently managed by MCUNED-Plus. The maps span over hundreds of meters, capturing a very high degree of materials heterogeneity and describing details in the range of millimeter size. The two more descriptive examples are the model of the tokamak complex [44,45] and the 360° model of the ITER tokamak, a computer model called E-lite [42]. The accurate characterization of the plasma radiation impinging on the bio-shield is a pre-requisite for the radiation mapping throughout the tokamak complex. This plasma radiation source for out-bioshield analyses has been modelled with a tailored computational methodology (SRC-UNED methodology) [42,46] and for the first time with a 360º model of the Tokamak [43]. Another relevant radiation source to be considered is that of the activated water. A novel workflow to produce detailed radiation source models of activated water has been developed at UNED [47]. Other approaches are in development at UNED for activation of fluids considering more realistic coolant flow patterns.

An example of nuclear analysis performed for DONES is the calculation of SDDR in the accelerator room. GEOUNED was used for generating the accelerator simulation model, and D1SUNED provided the SDDR mapping with an appropriate source modeling. Results showed the risk associated from steel line elements.

On the optimization of the pre-conceptual design of EUROfusion DEMO building, the tools developed at the UNED university have made possible the characterization of the residual dose fields. Special mention receives the radiological study performed for the ceramic materials considered in the high-temperature DEMO DCLL BB concept [48] and the issues of the activated water generated in the cooling systems of the WCLL and HCPB BB concepts, specially calculating some essential values for the protection of electronics and workers [49]. Besides, a study considering the presence of flowing activated PbLi has been done similarly to the above-mentioned study for water; the neutronics analysis performed on systems and pipelines conducting the alloy have been very useful for the planning of DEMO maintenance tasks.

4. Summary

For more than 10 years, development projects of materials with applications in magnetic and inertial confinement fusion and its associated technologies have been carried out within the framework of the TechnoFusión Programme. The programme comprises groups from the most prestigious universities (UPM, UNED, UCIIIM and UCM) and renowned research centers (CSIC and CMAM-UAM), coordinated by CIEMAT.

Numerous studies in the field of materials science and engineering have been undertaken as part of the Programme.

Materials with improved properties have been produced and characterized, focusing on obtaining more robust materials and components for the harsh conditions of future fusion reactors. To this aim, metallic materials with structural applications but also oxides and carbides as ceramic candidates for future breeding blankets have been manufactured and tested, paying special attention to guarantee their structural response and functionality under high radiation conditions. Although at an initial level, coatings and the result of their interaction with electron and ion radiation have also been addressed. Besides, cutting-edge technologies have been developed to predict the behaviour of materials and components, with the aim of bringing the studies closer to the conditions of future reactors. This is the case of studies of motorized components in high radiation areas, or of dose sensors on workers in complex radioactive facilities.

Furthermore, the construction of medium-sized facilities required for testing the functionality of materials and components under near-operational conditions has been addressed. The interest in establishing the chemical compatibility of materials in contact with PbLi and the testing of technologies associated with the extraction of T from the liquid alloy has led to the commissioning of two PbLi loops (CICLO and CLIPPER) working close to Breeding Blanket operating conditions. In the near future, CICLO is expected to be equipped with a new, more rapidly accessible sample inlet and complementary detectors for dissolved impurities in the liquid metal. In addition, a magnetic field will be incorporated to the studies of PbLi compatibility. On the other hand, CLIPPER has completed the commissioning phase using dummy sections, and will soon house the prototypes under development for permeation and H isotope injection technologies, to start testing under WCLL and DCLL conditions. The evolution of the triple ion beam facility and the timescale of its construction depend on administrative factors, now being concentrated in authorization procedures of the First Phase: the building of the two linear accelerators and the adequate protection of the building. In addition, the extraction of a mono-energetic neutron beam is planned in CID to neutron - ion material damage comparison and the calibration of fast neutron sensors. Simulating the neutron damage and the neutron transmuted by-products by using accelerated ion beams, the CID facility combining three ion beams (light and heavy elements) on double and triple irradiation chambers, characterized by variable currents (up to 10-40 µA) and low doses, is under construction.

Of particular importance in the design of complex facilities and in the estimation of parameters associated with radiation sources and radiation transport has been the development of neutronics. The TechnoFusión programme has accompanied this development in EUROfusion, applying its codes in the definition of complex facilities as ITER, IFMIF-DONES and DEMO, with the exciting conclusion that the DS1UNED is the reference code system in ITER for shutdown dose rate calculations.

Summarizing, the TechnoFusión consortium, formed by the most relevant Spanish institutions in the field of fusion, has been continuously funded from the Regional Government of Madrid, Spain, for the recruitment of the human team allowing the address of medium and long-term developments. In fact, the optimal achievement of the objectives of a scientific and technological project such as those proposed in TechnoFusión demonstrates the importance of having a powerful, ambitious and well-funded human network as a basis for tackling major challenges.

Declaration of Competing Interest

The authors declare that they have no known competing financial interests or personal relationships that could have appeared to influence the work reported in this paper.

CRediT authorship contribution statement

M. Gonzalez: Conceptualization, Investigation, Visualization, Writing – original draft, Writing – review & editing, Project administration. **R. Román:** Project administration, Conceptualization. **L. Bañares:** Conceptualization, Investigation, Supervision, Writing – review & editing. **M. Ferre:** Conceptualization, Investigation, Supervision, Writing – review & editing. **G. García:** Conceptualization, Supervision, Writing – review & editing. **R. González-Arrabal:** Conceptualization, Investigation, Supervision, Writing – review & editing. **A. Ibarra:** Conceptualization. **M.A. Monge:** Conceptualization, Investigation, Supervision, Writing – review & editing. **J. Olivares:** Conceptualization, Investigation, Supervision, Writing – review &

editing. **J.M. Perlado:** Conceptualization. **D. Rapisarda:** Conceptualization, Investigation, Supervision, Writing – review & editing. **F. Sánchez:** Conceptualization, Investigation, Supervision, Writing – review & editing. **J. Sanz:** Conceptualization, Software, Supervision, Writing – review & editing. **F. Seco:** Conceptualization, Investigation, Supervision, Writing – review & editing. **R. Vila:** Conceptualization, Investigation, Supervision, Writing – review & editing.

Acknowledgements

The authors acknowledge the funding by Community of Madrid, co-financed with Structural Funds (ERDF and ESF)), through the TechnoFusión (III)-CM (S2018/EMT-4437) programme, and the invaluable collaboration of the remaining members, staff and PhD students of the above-mentioned institutions, who can be found listed at http://projects.ciemat.es/web/programa-technofusion/participantes.

This work has also been carried out within the framework of the EUROfusion Consortium and has received funding from the European Union's Horizon 2020 research and innovation program under grant agreement number 633053. The views and opinions expressed in this document do not necessarily reflect those of the European Commission.

In particular, R. González-Arrabal acknowledges the Convenio Plurianual con la Universidad Politécnica de Madrid en la línea de actuación Programa de Excelencia para el Profesorado Universitario of the CAM (Comunidad Autónoma Madrid).

Supplementary materials

Supplementary material associated with this article can be found, in the online version, at doi:10.1016/j.jnucmat.2022.153854.

References

[1] M. Eddahbi, M.A. Monge, A. Muñoz, O.J. Dura, B. Savoini, Microstructure of a new ODS Cu–0.7wt-%Cr–0.11wt-%Zr material produced by a novel powder metallurgical method, Powder Metall. (2021), doi:10.1080/00325899.2021.1992135.
[2] A. Muñoz, B. Savoini, M.A. Monge, Y. Ortega, O.J. Dura, Fabrication and characterization of Cu reinforced with Y-enriched particles following a novel powder metallurgy route, Nucl. Mater. Energy 29 (2021) 101075, doi:10.1016/j.nme.2021.101075.
[3] A. Muñoz, B. Savoini, M.A. Monge, M. Eddahbi, O.J. Dura, Microstructure and mechanical properties of hot rolled ODS copper, Nucl. Mater. Energy 24 (2020) 100754, doi:10.1016/j.nme.2020.100754.
[4] G. Carro, A. Muñoz, B. Savoini, M.A. Monge, Fabrication and characterization of dispersion strengthened Cu-0.8%Y, Fusion Eng. Des. 154 (2020) 111548, doi:10.1016/j.fusengdes.2020.111548.
[5] Y. Zhang, History of high-entropy materials, in: High-Entropy Materials, Springer, 2019, pp. 1–33.
[6] E.J. Pickering, A.W. Carruthers, P.J. Barron, S.C. Middleburgh, D.E.J. Armstrong, A.S. Gandy, High-entropy alloys for advanced nuclear applications, Entropy 23 (2021) 98 28 pp, doi:10.3390/e23010098.
[7] N.A.P. Kiran Kumar, C. Li b, K.J. Leonard, H. Bei, S.J. Zinkle, Microstructural stability and mechanical behavior of FeNiMnCr high entropy alloy under ion irradiation, Acta Mater. 113 (2016) 230–244, doi:10.1016/j.actamat.2016.05.
[8] O.A. Waseem, H.J. Ryu, Powder metallurgy processing of a WxTaTiVCr high-entropy alloy and its derivative alloys for fusion material applications, Sci. Rep. 7 (2017) 1926, doi:10.1038/s41598-017-02168-3.
[9] D. Stork, et al., Materials R&D for a timely DEMO: Key findings and recommendations of the EU Roadmap Materials Assessment Group, Fusion Eng. Des. 89 (7–8) (2014) 1586–1594, doi:10.1016/j.fusengdes.2013.11.007.
[10] A. Rodriguez-Lopez, B. Savoini, M.A Monge, A. Muñoz, P. Pérez, Exploring CuCrFeVTi system to produce high entropy alloys for high heat flux applications, Nucl. Mater. Energy 29 (2021) 101065, doi:10.1016/j.nme.2021.101065.
[11] Y. Ortega, M.A. Monge, B. Savoini, A. Muñoz, P. Pérez, Production and characterization of the Cr35Fe35V16.5Mo6Ti7.5 high entropy alloy, Nucl. Mater. Energy (2022) 30, doi:10.1016/j.nme.2022.101148.
[12] A. Rodriguez-Lopez, B. Savoini, M.A Monge, A. Muñoz, Characterization and evaluation of CuCrFeV(Ti,Ta,W) system for High Heat Flux applications, Nucl. Mater. Energy 31 (2022) 101187, doi:10.1016/j.jnucmat.2015.11.044.
[13] M. Eddahbi, M.A. Monge, P. Carvalho, New high strength ODS Eurofer steel processed by mechanical alloying, Mater. Sci. Eng. A 817 (2021) 141288, doi:10.1016/j.msea.2021.141288.
[14] M. Oñoro, J. Macías-Delgado, M.A. Auger, V. de Castro, T. Leguey, Mechanical properties and stability of precipitates of an ODS steel after thermal cycling and aging, Nucl. Mater. Energy 24 (1-8) (2020) 100758, doi:10.1016/j.nme.2020.100758.
[15] M. Šćepanović, V.de Castro, I. García-Cortés, F.J. Sánchez, T. Gigl, C. Hugenschmidt, T. Leguey, Characterisation of open volume defects in Fe–Cr and ODS Fe–Cr alloys after He^{+} and Fe^{+} ion irradiations, J. Nucl. Mater. 538 (2020) 152230, doi:10.1016/j.jnucmat.2020.152230.
[16] M. Šćepanović, T. Leguey, I. García-Cortés, F.J. Sánchez, C. Hugenschmidt, M.A. Auger, V. de Castro, Sequential ion irradiations on Fe-Cr and ODS Fe-Cr alloys, Nucl. Mater. Energy 25 (2020) 100790, doi:10.1016/j.nme.2020.100790.
[17] W. Xu, L. Li, J.A. Valdez, M. Sabe, Y. Zhu, C.C. Koch, Effect of nano-oxide particle size on radiation resistance of iron-chromium alloys, J. Nucl. Mater. 469 (2016) 72–81, doi:10.1016/j.jnucmat.2015.11.044.
[18] N. Gordillo, M. Panizo-Laiz, E. Tejado, I. Fernandez-Martinez, A. Rivera, J.Y. Pastor, C.G. de Castro, J. del Rio, J.M. Perlado, R. Gonzalez-Arrabal, Morphological and microstructural characterization of nanostructured pure α-phase W coatings on a wide thickness range, Appl. Surf. Sci. 316 (2014) 1–8, doi:10.1016/j.apsusc.2014.07.061.
[19] T. Hernández, F.J. Sánchez, A. Moroño, E. León-Gutiérrez, M. Panizo-Laiz, M.A. Monclus, R. González-Arrabal, Corrosion behavior of diverse sputtered coatings for the helium cooled pebbles bed (HCPB) breeder concept, Nucl. Mater. Energy 25 (2020) 100795, doi:10.1016/j.nme.2020.100795.
[20] T. Hernández, A. Moroño, F.J. Sánchez, C. Maffiotte, M.A. Monclús, R. González-Arrabal, Study of deuterium permeation, retention, and desorption in SiC coatings submitted to relevant conditions for breeder blanket applications: thermal cycling effect under electron irradiation and oxygen exposure, J. Nucl. Mater. 557 (2021) 153219, doi:10.1016/j.jnucmat.2021.153219.
[21] A. Redondo-Cubero, M.J.G. Borge, N. Gordillo, P.C. Gutiérrez, J. Olivares, R. Pérez Casero, M.D. Ynsa, Current status and future developments of the ion beam facility at the centre of micro-analysis of materials in Madrid, Eur. Phys. J. Plus 136 (2021) 175, doi:10.1140/epjp/s13360-021-01085-9.
[22] J.M. Garcia, M. González, F. Sánchez, Comparative study of the mechanical properties after proton irradiation of Al2O3 and Si-SiC ceramics for fusion breeding blanket applications, Fusion Eng. Des. (2022).
[23] J.M. Garcia, M. González, M. Roldán, F. Sánchez, The microstructural in-sight to the mechanical behavior of alumina after high energy proton irradiation, Nucl. Mater. Energy 31 (2022) 101173, doi:10.1016/j.nme.2022.101173.
[24] G. Miccichè, M. Ascott, A. Bakic, D. Bernardi, J. Brenosa, S. Coloma, O. Crofts, G. Di Gironimo, M. Ferre, G. Fischer, A. Ibarra, A. Karap, I.G. Kiss, C. Kunert, L. Lorenzelli, G. Mitchell, M. Mittwollen, P. Pagani, S. Papa, G. Porempovics, T. Tadic, T. Matyas, The remote handling system of IFMIF-DONES, Fusion Eng. Des. 146 (2019) 2786–2790, doi:10.1016/j.fusengdes.2019.01.112.
[25] S. Coloma, M. Ferre, F. Arranz, G. Micciché, D. Sanchez-Herranz, O. Nomen, J.M. Cogollor, Remote handling maintenance of beam dump in IFMIF-DONES, Fusion Eng. Des. 165 (15–24) (2021) 112216, doi:10.1016/j.fusengdes.2020.112216.
[26] V. Tormo, F. Seco, A.R. Jiménez, Design of an RFID-based positioning system for safety of personnel in nuclear facilities, IEEE International Conference on Indoor Positioning and Indoor Navigation (IPIN), Lloret de Mar, Nov. 29 Dec 2, 2021.
[27] E. Carella, D. Rapisarda, S. Lenk, Design of the CIEMAT corrosion loop for liquid metal experiments, Appl. Sci. 12 (6) (2022) 3104, doi:10.3390/app12063104.
[28] B. Garcinuño, et al., The CIEMAT LiPb Loop permeation experiment, Fusion Eng. Des. 146 (2019) 1228–1232.
[29] B. Garcinuño, et al., Design and fabrication of a Permeator Against Vacuum prototype for small scale testing at Lead-Lithium facility, Fusion Eng. Des. 124 (2017) 871–875.
[30] M. Malo, et al., Experimental refutation of deuterium permeability in vanadium, niobium and tantalum, Fusion Eng. Des. 146 (2019) 224–227.
[31] B. Garcinuño, et al., Design of a system for hydrogen isotopes injection into Lead-Lithium, Fusion Eng. Des. 137 (2018) 427–434.
[32] G.S. Was, S. Taller, Z. Jiao, A.M. Monterrosa, D. Woodley, D. Jennings, T. Kubley, F. Naab, O. Toader, E. Uberseder, Resolution of the carbon contamination problem in ion irradiation experiments, Nucl. Instrum. Methods Phys. Res. Section B 412 (2017) 58–65, doi:10.1016/j.nimb.2017.08.039.
[33] J. García, J.P. Catalán, J. Sanz, Development of the automatic void generation module in GEOUNED conversion tool, Fusion Eng. Des. 168 (2021) 112366.
[34] P. Sauvan, J. Sanz, F. Ogando, New capabilities for Monte Carlo simulation of deuteron transport and secondary products generation, Nucl. Instrum. Methods Phys. Res. A 614 (2010) 323–330.
[35] P. Sauvan, J. Catalan, F. Ogando, R. Juarez, J. Sanz, Development of the R2SUNED code system for shutdown dose rate calculations, IEEE Trans. Nucl. Sci. 63 (2016) 375–384.
[36] P. Sauvan, R. Juárez, G. Pedroche, J. Alguacil, J.P. Catalan, F. Ogando, J. Sanz, D1SUNED system for the determination of decay photon related quantities, Fusion Eng. Des. 151 (2020) 111399.
[37] J. Alguacil, P. Sauvan, R. Juarez, J.P. Catalan, Assessment and optimization of MCNP memory management for detailed geometry of nuclear fusion facilities, Fusion Eng. Des. 136 (2018) 386–389.
[38] J. Alguacil, P. Sauvan, J.P. Catalan, J. Sanz, Development of a methodology to estimate the statistical SDR uncertainty with R2S-UNED, Fusion Eng. Des. 168 (2021) 112696.
[39] J. Sanz, O. Cabellos, N. García-Herranz, ACAB Innovatory Code for Nuclear Applications. Userś Manual V, Nuclear Energy Agency NEA Data Bank, 2008 NEA-1839/02, 2011.

[40] G. Pedroche, P. Sauvan, J. Alguacil, J. Sanz, R. Juárez, Nuclear data for D1SUNED for the study of ITER planned in-situ maintenance dose scenarios, Fusion Eng. Des. 170 (2021) 112646.
[41] V. Lopez, P. Sauvan, F. Ogando, Shutdown dose rates calculations due to light ions induced activation using D1S methodology, Fusion Eng. Des. 167 (2021) 112298.
[42] R. Juarez, J.P. Catalan, F. Ogando, A.J. Lopez-Revelles, P. Sauvan, S. Jakhar, E. Polunovskiy, M. Loughlin, J. Sanz, ITER plasma source and building modelling to produce radiation maps, Nucl. Fusion 58 (12) (2018) 126012.
[43] R. Juarez, G. Pedroche, M.J. Loughlin, R. Pampin, P. Martinez, M. De Pietri, J. Alguacil, F. Ogando, P. Sauvan, A.J. Lopez-Revelles, A. Kolsek, E. Polunovskiy, M. Fabbri, J. Sanz, A full and heterogeneous model of the ITER tokamak for comprehensive nuclear analyses, Nat. Energy 6 (2021) 150–157.
[44] J. López-Revelles, J.P. Catalán, A. Kolšek, R. Juárez, R. García, M. García, J. Sanz, MCNP model of the ITER Tokamak complex, Fusion Eng. Des. 136 (2018) 859–863.
[45] R. Juárez, P. Martínez, M. Loughlin, Y. Le Tonqueze, The MCNP model of the Tokamak Complex and its Surroundings for 2020 ITER Radiation Maps, 2020 Tokamak Complex MCNP Model Report - ITER_D_3FEA8J_v1.1.
[46] J.P. Catalan, F. Ogando, R. Juárez, P. Sauvan, G. Pedroche, J. Alguacil, J. Sanz, Development of radiation sources for nuclear analysis beyond ITER bio-shield: SCR-UNED code, Comput. Phys. Commun. 275 (2022) 108309.
[47] M. De Pietri, J. Alguacil, A. Kolsek, G. Pedroche, N. Ghirelli, E. Polunovskiy, M. Loughlin, Y. Le Tonqueze, J. Sanz, R. Juarez, Integral modelling of the ITER cooling water systems radiation source for applications outside of the Bio-shield, Fusion Eng. Des. 171 (2021) 112575.
[48] I. Palermo, J.M. Garcia, M. González, M. Malo, D. Rapisarda, Radiological characterization of ceramic materials considered for the HT-DCLL DEMO reactor, Nucl. Mater. Energy 30 (2022) 101136.
[49] I. Palermo, C. Bachmann, L. Di Pace, M. García, C. Gliss, D. Leichtle, N. Terranova, Radiation level in the DEMO tokamak complex due to activated flowing water: Impact on the architecture of the building, Fusion Eng. Des. 166 (2021) 112373.